Archives of Environmental Contamination and Toxicology
https://doi.org/10.1007/s00244-020-00788-x

Characterization of Trace Elements in Atmospheric Deposition Studied by Moss Biomonitoring in Georgia

O. Chaligava[1,2] · Sh. Shetekauri[2] · Wael M. Badawy[1,3] · Marina V. Frontasyeva[1] · I. Zinicovscaia[1,4] · T. Shetekauri[2] · A. Kvlividze[2] · K. Vergel[1] · N. Yushin[1]

Received: 4 May 2020 / Accepted: 12 November 2020

Abstract

The present work was conducted to obtain and highlight the first comprehensive baseline data on atmospheric deposition of trace elements and to evaluate the air quality in Georgia. A total of 120 moss samples were collected over accessible territories in Georgia in the period from 2014 to 2017. *Hylocomium splendens* (Hedw.) Schimp., *Hypnum cupressiforme* (Hedw.), and *Pleurozium schreberi* (Brid.) Mitt. moss species were analyzed by two complementary analytical techniques: instrumental neutron activation analysis and atomic absorption spectrometry. Concentrations of 41 elements in mg/kg were determined. The concentrations were compared with the corresponding values in the literature and are in a good agreement, except for the concentration of Mg, Al, K, Ca, Ti, and Fe, which were higher than those reported for other countries. The principal component and discriminant analyses were implemented to extract information about the similar geochemical features and to decipher the provenance of the studied elements. The analysis showed that a considerable association of crustal elements and the provenance of elements can be considered as a mixture of geogenic and anthropogenic sources. In addition, the influence of different latitudinal climate zones on the distribution of elements in the atmospheric deposition was observed. The enrichment factor shows considerable values for Th and Zr. The spatial distribution of the pollution load index identifies four zones (#12, 38, 53, and 64). The potential ecological risk index and the risk index were calculated and it does not pose significant risk except As and Cd. The data obtained can be used as the first dataset of metal characterization of air pollution in Georgia.

Air pollution is a serious worldwide problem caused by anthropogenic activities and is closely related to economics and human health. Air pollution consists of a mixture of gas, liquid, and solid compounds, which may pose a potential hazard to human health and cause detrimental changes to the biotic and abiotic components of the terrestrial ecosystem (Brunekreef and Holgate 2002; Kampa and Castanas 2008). Heavy metals are dangerous pollutants, because they are steady in the environment and can be easily accumulated in food chains. Metals are released to the environment from a wide range of anthropogenic and natural sources, such as mining, mechanical engineering, heavy and chemical industry, oil processing, deforestation, soil erosion, combustion of wood or agricultural waste, and land degradation (Hassanien 2011). Heavy metals are usually carried on fine particles, which also serve as a reaction layer for many heavy metals. They bind to the surface of dust particles, which leads to instability of the heavy metals and increases their biological activities (Acosta et al. 2015; Salim Akhter and Madany 1993; Yekeen et al. 2016).

Many studies have paid a great attention to the measurements of the concentration and determination of the heavy metals in Georgia. However, these studies were mainly devoted to the extraction of more information about the metal concentrations in soil, water, and food. Avkopashvili

Electronic supplementary material The online version of this article (https://doi.org/10.1007/s00244-020-00788-x) contains supplementary material, which is available to authorized users.

✉ Marina V. Frontasyeva
marina@nf.jinr.ru

[1] Frank Laboratory of Neutron Physics, Joint Institute for Nuclear Research, Dubna, Russian Federation 141980

[2] I. Javakhishvili Tbilisi State University, Chavchavadze ave. 3, Tbilisi 0179, Georgia

[3] Radiation Protection and Civil Defense Department, Nuclear Research Center, Egyptian Atomic Energy Authority (EAEA), 13759 Abu Zaabal, Egypt

[4] Horia Hulubei National Institute for Physics and Nuclear Engineering (IFIN-HH), Bucharest Magurele, Romania

Published online: 24 November 2020

et al. (2017) have determined the concentrations of Cu, Zn and Cd in soil, water, and food products in the vicinity of the gold and copper mine, Kazreti. Authors reported that the concentrations of the heavy metals in soil were observed to be up to 6000 mg/kg for Zn, 2000 mg/kg for Cu, and 100 mg/kg Cd, respectively, which suggests that this soil is practically useless for agriculture. In terms of industrial pollution of rivers of Georgia heavy metals play a significant role. The most toxic of them are: cadmium, copper, lead, zinc, manganese, and mercury. These toxic elements enter the aquatic environment as a result of the disposed untreated or uncontrolled industrial discharges. For many years, sewage has been flowing into the Mtkvari River, containing approximately 70 different substances (Lomsadze et al. 2016). The concentration of Cr, Cu, Mn, Ni, Pb, and Zn were determined in the soil of Western Georgia and considerable amounts of Mn, Cu, and Pb was noticed as it was reported by Gambashidze et al. (2014) and Urushadze et al. (2007). According to Caruso et al. (2012), the water quality is affected by a large amount of Mn, as one of the richest deposits of manganese (Mn), as well as mining areas are located in the foothills of the Caucasus Mountains, near the city of Chiatura in Georgia.

Likewise, another study was presented by Chirakadze et al. (2016) on the determination of As in soil and waste samples from Racha-Lower Svaneti district. High amounts of As was noticed (i.e., village Khoruldashi, As concentrations range from 61 to 170,000 mg/kg). Consequently, the elevated amounts of chemical elements may pose considerable impacts on humans. Therefore, the qualitative and quantitative identification of these elements will help to assess the air quality.

The traditional mechanisms of collection of atmospheric deposition using bulk-air sampler devices propose a practical method for air monitoring in terms of elemental composition. However, this approach has some limitations: for example, high cost, time-consuming, and need for technical support (Azimi et al. 2003; Saitanis et al. 2013). Alternatively, biomonitoring techniques are accepted methods to assess the metal air pollution. They depend on the accumulation of elements and radionuclides in biological materials, leaves of vascular evergreen plants, or tissues of nonvascular species, such as lichens or mosses (Saitanis et al. 2013). Mosses act as good biomonitors, because they have no roots and get their nutrients from the atmosphere. Therefore, large-scale biomonitoring surveys based on terrestrial moss have been conducted to assess the deposition of atmospheric pollutants (Allajbeu et al. 2016; Barandovski et al. 2015; Stafilov et al. 2018). Mosses obtain their nutrients from wet and dry deposition and are relatively independent of the substrate on which they grow. Although rhizoids externally look like roots, they cannot adsorb nutrients from the soil and only anchor the organism to a substrate. The weakly developed cuticle in moss tissues adduces to the accumulation of metals above their physiological needs (Allajbeu et al. 2016; Steinnes et al. 1992; Steinnes et al. 1997; Tessier and Boisvert 1999). The moss biomonitoring method is broadly employed by the International Cooperative Program on Effects of Air Pollution on Natural Vegetation and Crops, (UNECE ICP) Vegetation Programme (Georgia also participates since 2014), which publish their annual reports (Frontasyeva et al. 2020; Harmens et al. 2015).

Unfortunately, there is no widescale study in Georgia that studied the impact of heavy metals on the air quality. For the first time in Georgia, a baseline data of 41 elements in 120 moss samples covering almost the entire country (*Hylocomium splendens* (Hedw.) Schimp., *Hypnum cupressiforme* Hedw., and *Pleurozium schreberi* (Brid.) Mitt.), which were collected in different regions of Georgia within the period from 2014 through 2017, was comprehensively presented. The collected moss species were subjected and analyzed using two complementary analytical techniques: namely, instrumental neutron activation analysis (INAA) and atomic absorption spectroscopy (AAS). Therefore, the present work was conducted to achieve the following objectives and bridge this research gap: (i) determination of the abundances of trace elements and potentially toxic ones deposited in moss; (ii) quantification of the pollution extent using different indices (i.e., enrichment factor (EF), relative accumulation factor (RAF), potential ecological risk (PER) for some selected elements (Cr, Ni, Cu, Zn, As, Pb, and Cd), risk index (RI), and pollution load index (PLI)); (iii) determination of the accumulation of elements in different moss species during the period of 2014–2017 and extraction of information about the difference in concentrations per year; and (iv) delivery of the first comprehensive baseline data on the inorganic characterization of air quality in Georgia. This in turn can be considered as the beginning of a series of studies of air quality, which might help the regulatory bodies to set the necessary laws and rules that control the emission of trace elements in the atmosphere.

Materials and Methods

Study area

Georgia is a mountainous country with an area of 69,700 km^2. It is located in the Caucasus region within the collision zone of the Eurasian and Afro-Arabian plates, in the Mediterranean (Alpine-Himalayan) belt. Georgia's geographic coordinates are − 43° 35′ N latitude and 40°23′ E longitude for the North, − 41° 02′ N latitude and 46° 30′ E longitude for the South, − 43° 23′ N latitude and: 40° 00′ E longitude for the West, and latitude: 41° 17′ N latitude and 46° 44′ E longitude for the East. The relief of Georgia is

characterized by complex hypsometric and morphographic features: heavily dissected mountain slopes, deep erosive gorges, intermountain depressions, flat lowlands, plains, plateaus, and uplands. The most important landforms found in the territory of Georgia are erosive, volcanic, karst, gravitational, and old glacial landforms.

The climate in Georgia is extremely diverse, and the essential role in moderating it is played by the Greater Caucasus Mountain Range, which provides a buffer against the penetration of cold air masses from the north. The Greater Caucasus Range is characterized by erosive dissection and steep slopes, as well as older glacial landforms (troughs, circuses, and moraines) and karst formations (caves, dolines, and shafts). The Lesser Caucasus Mountains also help to shield against the influence of dry and hot air masses from the south. The Lesser Caucasus is characterized by a hilly and gorgy terrain. In some areas, the tower-shaped relief is associated with Eocene volcanic rocks; at certain locations, young volcanic formations are observed (Borjom-Bakuriani areas). The depth of erosion dissection varies between 500 and 1000 m on average. The Likhi Range, which connects the Greater and Lesser Caucasus, divides Georgia into Eastern and Western regions. Thus, there are two major climatic zones. In Western Georgia, the marine subtropical humid climate prevails with a total annual precipitation of 1200–2500 mm, whereas Eastern Georgia has a transitional climate from subtropical continental climate to marine humid one with a total annual precipitation of 530–1400 mm (Westen et al. 2012).

Sampling strategy

The most common moss species were used in the biomonitoring studies. The sampling area covered nine administrative regions of the country. A total of 120 samples of moss (*H. splendens* $n=34$, *H. cupressiforme* $n=64$, and *P. schreberi* $n=22$), growing on organic-rich surface soils in forests, foothills, subalpine, and alpine belts, and in other natural environments, were collected during the summer months of 2014–2017. The altitudes range from 161 m to 2763 m. The sampling localities are shown in Fig. 1. Details about moss species sampled in Georgia are given in Table 1.

The sampling was carried out according to the standard procedure described in the ICP Vegetation—Moss survey protocol (Harmens et al. 2015). The sampling sites were located at least 300 m from the main roads and populated

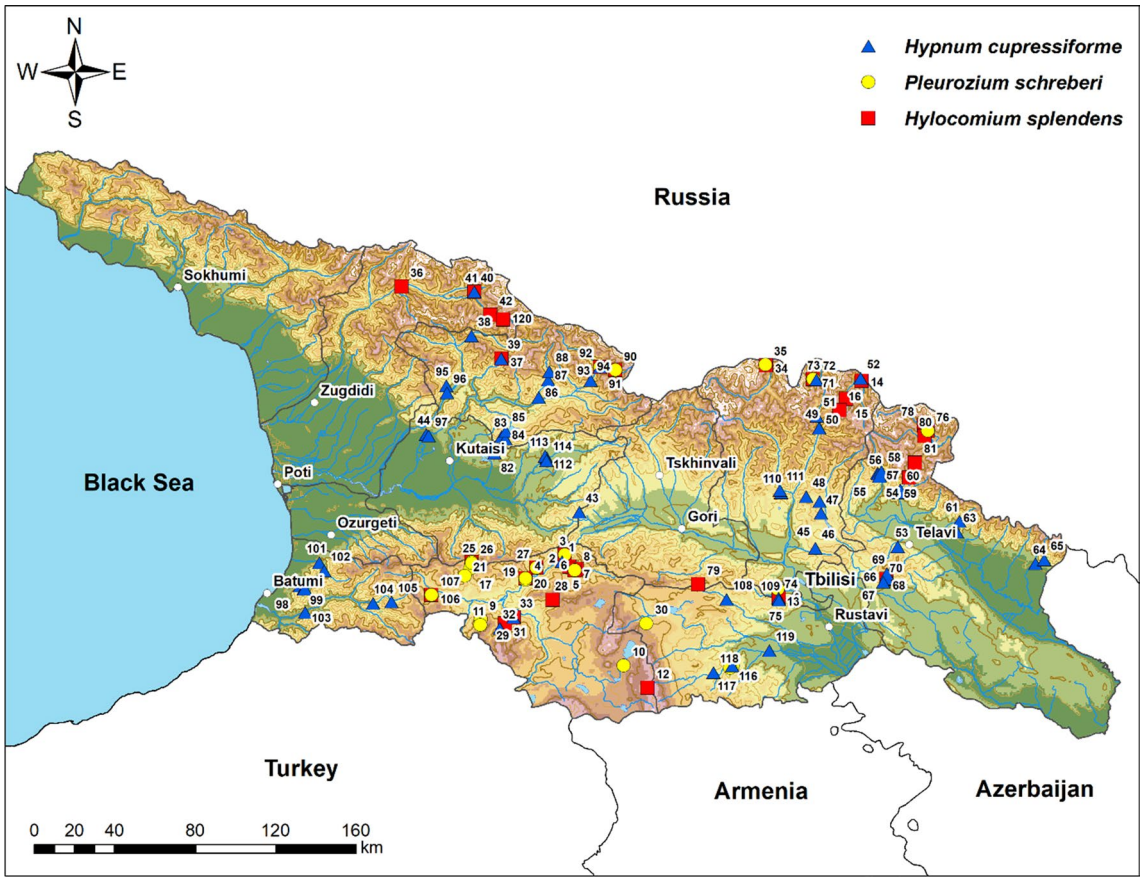

Fig. 1 Map of sampling localities

Table 1 Sampled moss species in Georgia

Regions (Administrative)	*H. splendens*	*P. schreberi*	*H. cupressiforme*	Total Samples
Adjara	–	–	8	8
Imereti	–	–	9	9
Kakheti	6	1	16	23
Kvemo Kartli	2	3	6	11
Mtskheta-Mtianeti	5	2	11	18
Racha-Lechkhumi and Kvemo Svaneti	3	2	10	15
Samegrelo-Zemo Svaneti	4	–	1	5
Samtskhe-Javakheti	14	13	3	30
Tbilisi	–	1	–	1
Total	34	22	64	120

areas and at least 100 m away from smaller roads or single houses. The sampling points were situated at least 3 m away from the nearest tree canopy. Moss samples were collected in appropriate amounts (approximately 1 litre) dependent on the availability and accessibility. For each sampling site, 5–10 subsamples were taken within a 2500-m^2 area and mixed to one representative sample. Descriptions of all sites were recorded for future use together with the geographical coordinates determined by Global Positioning System (GPS) and the time of the sampling. Each sampling site was photographed and archived.

Moss preparation

Sample preparation was performed in a chemical laboratory. Plastic tweezers and disposable polyethylene gloves were used to prevent contamination of the material. Each sample was cleaned from extraneous materials. Only green and green–brown shoots were taken. They were dried to a constant weight at 30–40 °C for 48 h (Steinnes et al. 1994). The samples were measured and analyzed in the same year of sampling.

For instrumental neutron activation analysis (INAA), approximately 0.3 g of mosses were pelletized in press-forms. Then the samples were precisely weighed. Moss samples for short-term irradiation were heat-sealed in polyethylene foil bags, whereas the samples for long-term irradiation were packed in aluminum cups.

For atomic absorption spectrometry (AAS), approximately 0.2 g of moss was placed in a Teflon vessel and digested with 3 mL of concentrated nitric acid (HNO_3) and 2 mL of hydrogen peroxide (H_2O_2) in a microwave digestion system (Mars; CEM, Matthews, NC) for complete digestion. Digestion was performed in two steps: 1) ramp: temperature 160 °C, time 15 min, power 400 W, and pressure 20 bar; 2) hold: temperature 160 °C, hold time 10 min, power 400 W, and pressure 20 bar. Digests were quantitatively transferred to calibrated 100-mL flasks and made up to the volume with bidistilled water. All of the reagents used for this study were of analytical grade: nitric acid—69%; trace pure (Merck, Darmstadt, DE); hydrogen peroxide—30%, p.a. (Merck); and bidistilled water.

Analytical techniques

Instrumental neutron activation analysis (INAA)

Moss samples were subjected to the neutron activation analysis at the experimental installation REGATA of the IBR-2 reactor of Frank Laboratory of Neutron Physics, Joint Institute for Nuclear Research FLNP, JINR (Dubna, Russia). The samples were irradiated in the channels equipped with a pneumatic system installed at the IBR-2 pulsed nuclear reactor of FLNP with the average power of 2 MW. The main characteristics of the irradiation channels are published by Frontasyeva and Pavlov (2005). To determine the elements with short-lived isotopes (SLI) (Mg, Al, Cl, Ca, Ti, V, Mn, I) in the moss samples, each sample was irradiated for 3 min and measured for 15 min. Similarly, the long-lived isotopes were irradiated for 3 days in the Cd-screened channel under the neutron flux of 1.8×10^{11} n/cm^2 s. The samples were repacked and measured twice. The first measurement was performed for 30 min after 4 days of decay, and a set of elements was determined. These were the so-called first long-lived isotopes (LLI1) (Na, K, As, Br, Mo, La, Sm, W, Au, and U). The second one was performed for 1.5 h after 20 days of decay, and another set of elements was determined (Sc, Cr, Fe, Co, Ni, Zn, Se, Rb, Sr, Zr, Sb, Cs, Ba, Ce, Nd, Eu, Tb, Yb, Hf, Ta, Th), called second long-lived isotopes (LLI2).

Gamma spectra of the samples were measured by HPGe detector with a resolution of 2.5–3 keV for the 1332 keV line of the ^{60}Co. The Genie 2000 software was used to store, display, and analyze the gamma spectra. The other software

developed at FLNP was used to calculate concentrations of the elements in the samples. The analytical errors of the concentrations of the elements of interest range from 3 to 15%.

Atomic absorption spectrometry (AAS)

The (AAS) as a complementary tool was used to determine concentrations of Cu, Cd, and Pb in the moss samples using the iCE 3300 (AAS) atomic absorption spectrometer with electrothermal (graphite furnace) atomization (Thermo Fisher Scientific, Waltham, MA). The calibration solutions were prepared from a 1 g/l of stock solution (AAS standard solution; Merck, DE).

Quality control of (INAA) and (AAS)

The quality control of the (NAA) measurements was carried out using standard reference materials NIST SRM 1547-Peach Leaves, NIST SRM 1575a- Pine Needles, NIST SRM 1633b—Coal Fly Ash, NIST SRM1632c—Coal (Bituminous), NIST SRM 2709—San Joaquin Soil, and IRMM SRM 667—Estuarine Sediment. SRM varied between 1 and 14% with the exception of Mn, Ti, Mg, Br, Hf, Se, and Ca for which the relative differences were 20%. The neutron activation analysis data for the obtained and certified values of the reference materials are given in Table 2.

While the quality control of (AAS) was performed using the standard reference materials NIST SRM 1515 (Apple leaves), NIST SRM 1573 (Tomato leaves), SRM 1570a (spinach leaves), and SRM 1575a (pine needles). The difference between the certified and measured elements contents of the certified material varied between 1 and 5%. A comparison of heavy metal concentrations obtained using the (AAS) with the standard values are presented in Table 3.

Statistical data analysis

With 95% probability ($p \leq 0.05$), the Shapiro–Wilk test of normality (Shapiro and Wilk 1965) was calculated for the entire set of elements to investigate whether the concentrations of the elements are normally distributed. The equality of mean, median, and mode values suggests a normal distribution and the results are not skewed. The vast majority of statistical methods is based on the assumption of a normal distribution in the data entered. Based on that, a great attention should be paid when using these statistical methods with nonnormally distributed data this could give biased or even faulty results. Therefore, the implementation of normality test helps to check whether further statistical treatment of the data is needed (i.e., log transformation of the data) (Reimann and Filzmoser 2000).

Table 3 Comparison of the AAS-obtained heavy metal concentrations with the standard values, mg/kg

Element	Certified	Obtained
Cd	0.537 ± 0.02	0.54 ± 0.01
Cu	5.05 ± 0.10	4.60 ± 0.3
Pb	0.20 ± 0.06	0.18 ± 0.01

Table 2 NAA-obtained and certified values of reference materials, mg/kg

Element	Obtained	Certified	Element	Obtained	Certified
Na	10,900 ± 325	11,600 ± 302	Sr	55.7 ± 4.2	63.8 ± 1.4
Mg	1369 ± 188	1200 ± 30	Mo	0.83 ± 0.26	0.8 ± 0.24
Al	222 ± 12.7	249 ± 7.97	Sb	0.99 ± 0.07	0.96 ± 0.05
Cl	1120 ± 150	1139 ± 41.0	I	11.2 ± 2.3	11 ± 3.3
K	1023 ± 130	1100 ± 33.0	Cs	7.7 ± 0.3	7.8 ± 0.7
Ca	18,500 ± 5300	15,100 ± 604	Ba	800 ± 45	707 ± 50.9
Sc	13.9 ± 0.4	13.7 ± 0.70	La	34.6 ± 1.3	34 ± 10.2
Ti	422 ± 62	517 ± 32.1	Ce	183 ± 13.7	180 ± 54.0
V	0.36 ± 0.035	0.37 ± 0.03	Nd	82 ± 29.4	87 ± 26.1
Cr	187 ± 11.4	178 ± 16.0	Sm	19 ± 1.73	19 ± 5.70
Mn	10.7 ± 1.6	13.04 ± 0.52	Eu	0.12 ± 0.032	0.12 ± 0.0033
Fe	35,300 ± 1800	33,800 ± 1014	Tb	0.71 ± 0.02	0.68 ± 0.017
Co	41.6 ± 2.5	42.9 ± 3.52	Yb	1.58 ± 0.11	1.6 ± 0.48
Ni	132 ± 12	132 ± 10.0	Hf	2.83 ± 0.85	3.2 ± 0.96
Zn	184 ± 8	175 ± 13.0	Ta	0.84 ± 0.03	0.88 ± 0.018
As	5.4 ± 0.4	6.18 ± 0.27	W	93 ± 28.2	93 ± 27.9
Se	0.62 ± 0.12	0.78 ± 0.04	Au	0.6 ± 0.18	0.6 ± 0.18
Br	53.7 ± 6.44	67 ± 7.97	Th	10.3 ± 0.33	10 ± 0.50
Rb	107 ± 19	96 ± 28.8	U	2.49 ± 0.14	2.26 ± 0.15

Tukey test was performed to differentiate between the mean values of the accumulated concentrations of elements in different moss species and sampling years. In order to avoid the substantial differences between the concentrations of the determined elements, which leads to the nonnormal distribution of the data, the Box-Cox transformation was used to improve and boost the normality of the data (Barandovski et al. 2015; Box and Cox 1964).

One of the most powerful statistical analytical methods that is widely used to extract information about the origin of the determined elements is the discriminant analysis (DA). The discriminant analysis is a way to build classifiers and an attempt to identify the boundary between the groups in the dataset, which can then be used to classify new observations (Hallinan 2012).

Bivariate and multivariate statistical analyses of the data were performed using R: A Language and Environment for Statistical Computing (R Core Team 2016). The principal component analysis (PCA) function of the FactoMineR package was used (Lê et al. 2008). The software package Excel was used to handle and manage the data. (PCA), discriminant and visualizing of the results were performed using R environment for programming (Hamilton and Ferry 2018; Wickham 2016). The geographic information system (GIS) technology was used to map, by means of ArcGIS, the spatial distribution of the pollution patterns. The data were interpolated on the basis of the inverse distance weighting (IDW) method.

Before the implementation of (PCA) analysis, the raw data were centered log-ratio transformed (CLR). The centered log-ratio transformation (CLR) allows an excellent approximation in centering and presentation of the data. Next, the dataset was simplified into a lower dimensional space by using (PCA) and clustered using K-means methods. K-means method of clustering aims to partition the observations into K clusters, in which each observation belongs to the cluster with the nearest mean. Then, the data of (PCA) was plotted and visualized. To perform (PCA), 29 of 41 elements were selected. The others were eliminated from the matrix due to their tendency to form separate groups (outliers), thus not showing a reasonable link with other chemical elements.

Quantifying the pollution extent

Heavy metal pollution was assessed using various indices. Pollution indices are widely used as a useful tool for the integrative evaluation of the degree of contamination. In addition, they can be of great value in assessing air quality and predicting future ecosystem sustainability. Five indices, previously described by several authors, were calculated and compared (enrichment factor [EF], relative accumulation factor [RAF], pollution load index [PLI], potential ecological risk index [PER], and risk index [RI]) (Kowalska et al. 2016; Kowalska et al. 2018).

Enrichment factor

The EF is widely used to differentiate between the levels of the anthropogenic and geogenic metal pollution. The EF gives the characteristics of the elements in terms of enrichment or depletion in the samples under investigation. In the present work, the EF was calculated by using Fe as the reference element, because it is a "conservative" immobile element (Chen et al. 2007; Karuppasamy et al. 2017). The Fe concentration in the reference plant RF reported by Markert (1992) was used as a background to calculate the EF. The enrichment factor is categorized into seven classes as follows: $EF < 1$ is no enrichment; $1 \le EF < 3$ is minor enrichment; $3 < EF < 5$ is moderate enrichment; $5 < EF < 10$ is moderately severe enrichment; $10 < EF < 25$ is severe enrichment; $25 < EF < 50$ is very severe enrichment; and > 50 is extremely severe enrichment (Abrahim and Parker 2008; Badawy et al. 2020; Badawy et al. 2018; Badawy et al. 2017; Ergin et al. 1991; Lv et al. 2015; Madadzada et al. 2019; Reimann and de Caritat 2005). The EF is calculated using Eq. (1):

$$\mathrm{EF} = \left(C_x/C_{\mathrm{Fe}}\right)_{\mathrm{moss}} / \left(C_x/C_{\mathrm{Fe}}\right)_{\mathrm{reference}} \quad (1)$$

where $(C_x/C_{\mathrm{Fe}})_{\mathrm{moss}}$ is the ratio between the concentration of the element in the sample and the concentration of Fe in the sample while $(C_x/C_{\mathrm{Fe}})_{\mathrm{reference}}$ is the ratio of the corresponding element in reference plant to the Fe concentration reported by Markert (1992).

Relative accumulation factor (RAF)

To assess the element accumulation in the moss studied, the relative accumulation factor (RAF) was calculated using the following formula (Goryainova et al. 2016):

$$\mathrm{RAF} = \left(C - C_{\mathrm{reference}}\right)/C_{\mathrm{reference}} \quad (2)$$

where C is the initial element concentration, and $C_{\mathrm{reference}}$ is the corresponding element concentration in the reference plant reported by Markert (1992).

Pollution load index

The PLI is an easy approach to calculate the pollution load of the accumulated metals. PLI gives the integrative pollution assessment of the studied areas. It is calculated as the n*th* root of the product of n the pollution index (PI) (Kowalska et al. 2018; Varol 2011).

$$\mathrm{PLI} = \sqrt[n]{\prod_{i=1}^{n} \mathrm{PI}_i} \tag{3}$$

where n is the number of analyzed metals, and PI is the calculated values of the single pollution index for each metal. PI is the concentration of each individual element divided by the corresponding value of the same element in reference plant RF (Markert 1992). When PLI > 1, it means that pollution exists. Otherwise, if PLI < 1, there is no metal pollution.

Potential ecological risk index

The PER was used as a diagnostic tool for air pollution control purposes and for sorting out which investigated areas should be given a special attention (Hakanson 1980). PER was calculated for some selected elements that have "toxic-response" data in the literature. The formula of PER_f^i for a single metal pollution is

$$\mathrm{PER}_f^i = C_f^i \times T_f^i \tag{4}$$

where PER_f^i is the potential ecological risk index, C_f^i is the contamination factor, and T_f^i is the "toxic-response" coefficient for the given single metal. The corresponding T_f^i values are Zn = 1, As = 10, Cr = 2, Pb = Ni = Cu = 5, and Cd = 30 (Badawy et al. 2018; Hakanson 1980).

Risk index

Risk index, a single-entity index combining all of the metals of interest, is calculated as

$$\mathrm{RI} = \sum \mathrm{PER}_f^i \tag{5}$$

where RI is the sum of PER_f^i for each metal of interest (Hakanson 1980). The interpretation categories for RI are given in Table 4SM (Badawy et al. 2018; Hakanson 1980; Karuppasamy et al. 2017).

Results and Discussion

Many researchers have suggested different approaches to normalize the data prior to further analysis. For instance, Zhou et al. (2017) recommended considering as a background the average value of the minimum three values for each element in the site studied. Other researchers recommended using the corresponding values reported by Markert (1992) for a reference plant RP as did Abdusamadzoda et al. (2019), whereas Allajbeu et al. (2016) and Carballeira et al. (2002) used the average values reported in the literature from pristine or protected areas as a background. The concentrations in the collected samples from the protected areas are in line with the corresponding concentrations of other sampling sites. Therefore, the concentrations in these samples could not be considered as a background.

The normalization according to the first and second approaches was implemented, as illustrated in Figs. 2 and 3.

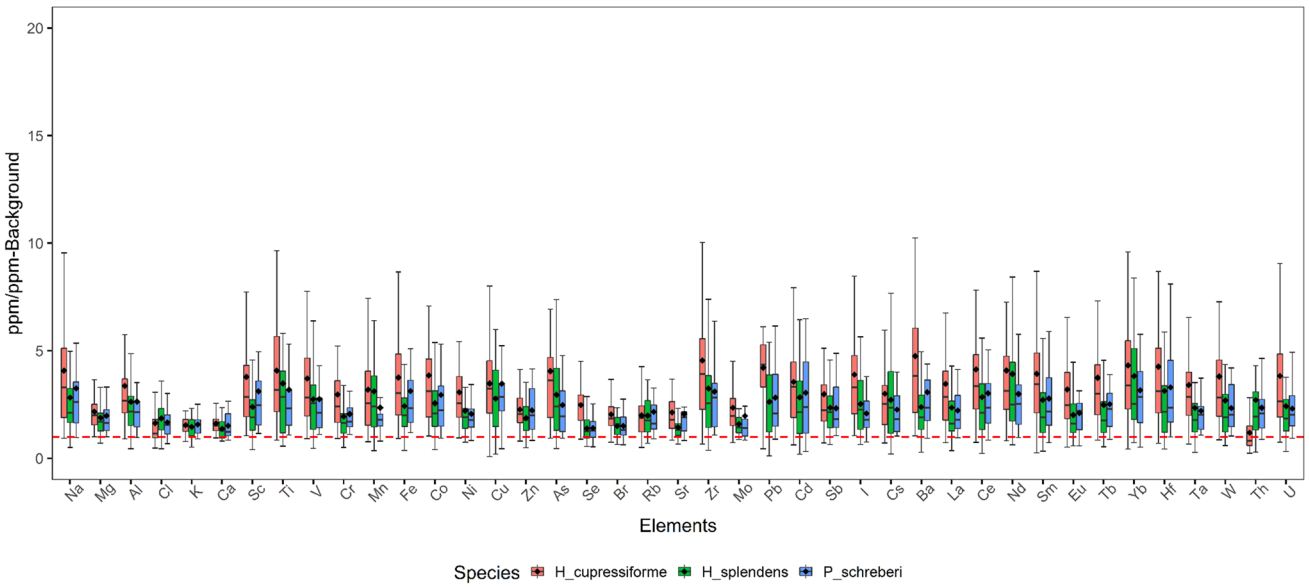

Fig. 2 Boxplot illustrating the to the normalized concentrations of elements to the average value of the minimum three values of each element for each species (Background) (*P. schreberi* PS, *H. cupressiforme* HC, and *H. splendens* HS). The dashed red line is the normalizing line

As illustrated in Fig. 2, the concentrations of the obtained elements normalized to the corresponding values of the average value of the minimum three values of each element (Background). While Fig. 3 illustrates the normalized concentrations of elements to the reference plants (RP) (Markert 1992). In the first approach, it was noticed that all the elements are quite high above the background, which, in turn, misleads and overestimates the obtained results. The values normalized to the corresponding values of the reference plant RP are in good agreement with the obtained results. To sum up, the approaches that we have used confirmed that normalization of the moss results to the corresponding values of the reference plant is the most appropriate in our case.

Abundances and intercorrelation of elements

Two complementary analytical techniques, (INAA) and (AAS), have been employed to extract the concentrations of 41 trace elements in 120 moss samples. The full descriptive statistics of 41 elements in all the moss species are shown in Table 4. The descriptive statistics in terms of the type of moss species are given in Tables 1SM, 2SM, and 3SM. (Suppl. Material). The findings of the normality test revealed that almost all of the elements are not normally distributed and therefore, further statistical treatment is needed. All of the results were normalized relative to the corresponding values for (RP) given by Markert (1992). The normalized results are illustrated in Fig. 3 and discriminated by the moss species. A boxplot illustrates the normalized concentrations of 40 major and trace elements determined in three types of the mosses studied (*P. schreberi* PS, *H. cupressiforme* HC, and *H. splendens* HS). The results of the normalized concentrations revealed that the concentrations of Al, Sc, Ti, V, Fe, As, Zr, Ta, Th, and rare earth elements (La, Ce, Sm, Eu, Tb, and Yb) are significantly high. The mean concentration value and standard deviation of Al in (mg/kg) was measured to be 5137 ± 3706 and ranges from a minimum value of 759 to a maximum value of 24,500 were noticed for #23 (Abastumani District, Zekari Pass) and #114 (Imereti, Chiatura), respectively.

Imereti, Chiatura is characterized by the existence of mining areas of Mn. This can explain the high contribution of these elements. Therefore, the highest concentration of Mn (2530, 2470, and 2010 mg/kg) was noticed in Imereti, Chiatura (mining areas) in #113, #114, and #112, respectively. These measurements were performed in 2017. In other years, the results show no significant pollution as illustrated in Fig. 1SM. This feature can be explained by the fact that in other years no samples were collected from these sites. It was reported by Boquete et al. (2011) that biomonitoring based on terrestrial mosses is not a reliable tool for assessment of the atmospheric manganese deposition. Only under certain circumstances and for certain types of emission, elevated concentrations of Mn will be observed in moss tissues due to the increased deposition of the element. Therefore, in the present work, terrestrial moss can be accepted as biomonitor, because the obtained concentrations of Mn are quite high. Mostly, the elevated content is due to the parent rock and several open-pit mines.

In addition, high concentrations of As were observed in one single location #87 with a mean concentration value of 83.30 mg/kg. The elevated concentration of As in this

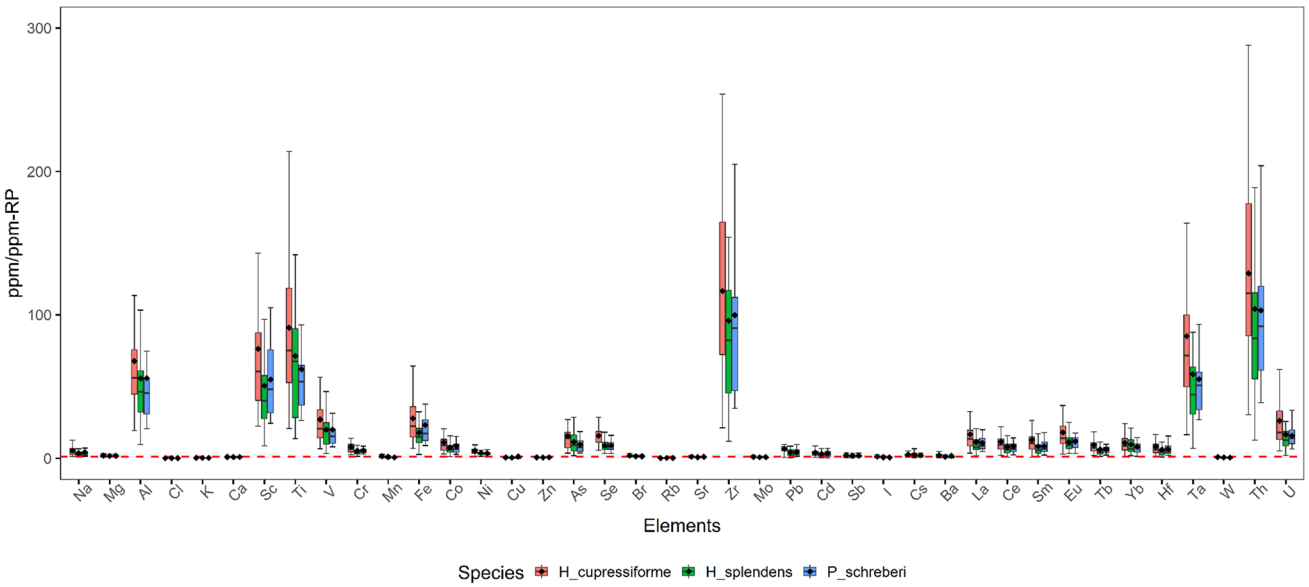

Fig. 3 Boxplot illustrating the normalized concentrations of 40 major and trace elements determined in three types of mosses studied (*P. schreberi* PS, *H. cupressiforme* HC, and *H. splendens* HS). The dashed red line is the normalizing line

Table 4 Descriptive statistics of the obtained element concentrations in the analyzed moss samples (n = 120)

Element	Mean ± SD	Median ± SD_Med	Geomean ± SD_geo	Min–Max	CV %	RAF	Skewness	Kurtosis	Statistic	*p* value	RP
Na	713.37 ± 503.04	581 ± 235	576.97 ± 1.92	101–30,00	71	3.76	1.65371	3.27865	0.84056	4.75E−10	150
Mg	3545.33 ± 1682.2	3060 ± 770	3233.74 ± 1.52	1220–11,600	47	0.77	1.80449	4.72179	0.85666	2.06E−09	2000
Al	5137.41 ± 3706.74	4295 ± 1500	4272.39 ± 1.8	759–24,500	72	63.22	2.55262	8.50391	0.75119	5.61E−13	80
Cl	220.35 ± 150.16	185 ± 63.5	188.89 ± 1.71	57.3–1080	68	-0.89	3.2645	15.14682	0.70856	4.04E−14	2000
K	5966.83 ± 1862.24	5935 ± 1245	5688.78 ± 1.37	2030–15,000	31	− 0.69	0.9961	3.41798	0.94909	1.85E−04	19000
Ca	8830.58 ± 2882.09	8255 ± 2050	8389.87 ± 1.38	4620–17,100	33	− 0.12	0.67956	− 0.23086	0.94779	1.49E−04	10000
Sc	1.39 ± 1.09	1.11 ± 0.4	1.11 ± 1.9	0.17–6.58	78	68.27	2.35537	6.79282	0.75548	7.43E−13	0.02
Ti	458.24 ± 377.7	349.5 ± 170.5	350.79 ± 2.06	68.6–2100	82	90.65	2.12086	5.52603	0.7866	6.40E−12	5
V	11.91 ± 8.92	9.4 ± 4.12	9.54 ± 1.93	1.71–54	75	22.81	2.00781	5.00371	0.80493	2.52E−11	0.5
Cr	10.16 ± 6.57	7.75 ± 2.65	8.66 ± 1.73	2.04–39	65	5.77	1.97603	4.65558	0.80292	2.16E−11	1.5
Mn	238.16 ± 366.41	141 ± 54.7	157.53 ± 2.19	21.7–2530	154	0.19	5.02244	27.54633	0.42478	0	200
Fe	3630.98 ± 2598.72	2725 ± 1050	2957.51 ± 1.88	404–14,100	72	23.21	1.84566	3.66528	0.81245	4.54E−11	150
Co	1.93 ± 1.45	1.43 ± 0.61	1.55 ± 1.91	0.23–8.12	75	8.63	1.97007	4.24287	0.79114	8.92E−12	0.2
Ni	6.81 ± 4.07	5.56 ± 1.8	5.91 ± 1.68	1.92–24.2	60	3.54	1.81269	3.96331	0.83189	2.24E−10	1.5
Cu	7.04 ± 13.15	5.54 ± 2.26	4.54 ± 2.64	0.13–143.07	187	− 0.30	9.49837	98.29329	0.26157	0	10
Zn	31.57 ± 12.96	28.85 ± 8.9	28.97 ± 1.53	7.15–75.2	41	− 0.37	0.75009	0.44706	0.96034	0.00135	50
As	2.02 ± 7.56	1.05 ± 0.56	1.07 ± 2.23	0.18–83.3	375	19.16	10.6038	114.7391	0.1387	0	0.1
Se	0.25 ± 0.13	0.23 ± 0.09	0.22 ± 1.67	0.07–0.65	50	11.48	0.86711	0.34995	0.93086	1.09E−05	0.02
Br	6.63 ± 2.95	6.31 ± 1.46	6.1 ± 1.51	2.33–25.2	44	0.66	2.41853	12.54903	0.84198	5.38E−10	4
Rb	11.63 ± 6.36	10.55 ± 3.56	10.23 ± 1.65	2.92–34.2	55	− 0.77	1.57056	2.84324	0.86158	3.30E−09	50
Sr	50.23 ± 25.19	43.85 ± 12.85	45.34 ± 1.56	17.2–157	50	0.00	1.77915	4.20235	0.84879	9.93E−10	50
Zr	13.05 ± 10.7	10.55 ± 5.32	9.89 ± 2.13	1.19–67.9	82	129.48	2.23842	6.96732	0.79815	1.50E−11	0.1
Mo	0.42 ± 0.27	0.35 ± 0.1	0.36 ± 1.63	0.15–2.1	66	− 0.17	3.20043	14.40778	0.70184	2.74E−14	0.5
Pb	5.46 ± 3.23	5.57 ± 2.33	4.32 ± 2.2	0.18–19.1	59	4.46	0.85092	2.08246	0.93722	2.79E−05	1
Cd	0.18 ± 0.12	0.15 ± 0.07	0.14 ± 2.12	0.01–0.58	68	2.51	1.26416	1.6686	0.8993	1.81E−07	0.05
Sb	0.2 ± 0.16	0.16 ± 0.06	0.17 ± 1.72	0.05–1.36	80	1.03	4.52246	27.61982	0.59996	1.67E−16	0.1
I	2.9 ± 1.99	2.48 ± 1.09	2.38 ± 1.86	0.58–11.8	69	− 0.03	1.89454	4.69954	0.83198	2.26E−10	3
Cs	0.49 ± 0.35	0.42 ± 0.19	0.4 ± 1.92	0.04–2.67	73	1.43	2.64463	11.89204	0.78823	7.21E−12	0.2
Ba	69.95 ± 57.56	51.3 ± 23.75	53.69 ± 2.06	4.98–365	82	0.75	2.16632	6.22943	0.78594	6.11E−12	40
La	2.82 ± 2.11	2.15 ± 0.91	2.28 ± 1.89	0.34–12	75	13.10	2.21764	6.19649	0.77885	3.67E−12	0.2
Ce	5.02 ± 3.79	3.75 ± 1.75	3.97 ± 2	0.32–21.7	75	9.04	2.05332	5.37862	0.80899	3.46E−11	0.5
Nd	2.75 ± 2.11	2.04 ± 0.87	2.18 ± 1.96	0.45–10.7	77	ND	1.92157	3.76999	0.79223	9.67E−12	ND
Sm	0.43 ± 0.37	0.34 ± 0.16	0.33 ± 2.13	0.03–2.74	86	9.75	2.97129	13.74868	0.74646	4.13E−13	0.04
Eu	0.12 ± 0.08	0.1 ± 0.04	0.1 ± 1.83	0.02–0.52	67	14.01	2.01272	5.78209	0.82681	1.46E−10	0.008
Tb	0.06 ± 0.05	0.05 ± 0.02	0.05 ± 1.92	0.01–0.31	76	6.93	2.19314	6.50139	0.79227	9.70E−12	0.008
Yb	0.2 ± 0.15	0.15 ± 0.07	0.16 ± 2.07	0.02–0.8	74	8.99	1.62443	2.80607	0.84755	8.87E−10	0.02

Table 4 (continued)

Element	Mean ± SD	Median ± SD_Med	Geomean ± SD_geo	Min–Max	CV %	RAF	Skewness	Kurtosis	Statistic	*p* value	RP
Hf	0.36 ± 0.29	0.27 ± 0.13	0.28 ± 2.05	0.04–1.81	81	6.23	2.104	5.93694	0.7952	1.21E−11	0.05
Ta	0.07 ± 0.05	0.06 ± 0.02	0.06 ± 1.88	0.01–0.28	71	71.15	1.92533	4.37728	0.81271	4.64E−11	0.001
W	0.14 ± 0.11	0.11 ± 0.04	0.11 ± 1.93	0.03–0.67	80	−0.29	2.24333	5.92167	0.76164	1.12E−12	0.2
Th	0.7 ± 0.55	0.51 ± 0.23	0.56 ± 1.96	0.06–2.9	78	139.70	2.13397	5.42316	0.78124	4.35E−12	0.005
U	0.21 ± 0.17	0.16 ± 0.07	0.17 ± 1.95	0.02–1.25	81	20.49	2.67711	10.88495	0.75344	6.49E−13	0.01

location is mainly due to the As mining area in Kvemo Racha, Ambrolauri district, in the environs of the village Uravi. This measurement was performed in 2016. However, all other As measurements show no anomalies. The mean value of As was measured as 2.02 ± 7.56 and ranges from a minimum value of 0.18 to a maximum value of 83.30 mg/kg. The mean concentration value and standard deviation of Sc is 1.38 ± 1.09 and with a range of 0.17–6.58 mg/kg were noticed for #23 and #100, respectively. The location of the highest contribution was observed in the south of Colchis, autonomous republic of Adjara, Kobuleti district, environs of village Chakvistavi.

The average value of Ti in (mg/kg) is 458.24 ± 377.70 and ranges from a minimum value of 68.59 to a maximum value of 2100. The minimum and maximum values were noticed for #93 and #82, respectively. The highest concentration of Ti was observed in the west of Georgia, Imereti region, Tkibuli district, in the environs of the town Tkibuli. These peculiarities can be explained by the impact of coal mining in Tkibuli. The mean value of Fe in (mg/kg) is 3630.983 ± 2598.72 and with a range of (404–14,100) were noticed for #23 and #8, respectively. The highest concentration of Fe was noticed in Lesser Caucasus. Borjomi District. To a great extent, the elevated amounts of Fe in the samples are mainly due the association of upper continental crustal Fe element.

Similarly, a significant contribution was observed from Co. The mean value of Co is 1.92 ± 1.45 with a minimum value of 0.23 and a maximum value of 8.12 were noticed for #23 and #100, respectively. The highest concentration was observed in the west of Georgia, the south of Colchis, autonomous republic of Adjara, Kobuleti district, environs of village Chakvistavi. The absence of potential sources of pollution in this vicinity suggests earth crustal weathering of Co. The concentration of Zr was significantly high relative to other elements where the mean value was measured to be 13.05 ± 10.69 and ranges from a minimum value of 1.19 to a maximum value of 67.9 were noticed for #24 and #83, respectively. Locations of maximum values of Zr, As, Th, and U is close to coal mining in Tkibuli (#83). This explains the elevated concentrations of these elements.

At the first glance at Fig. 1SM, one can realize that the elements of high contributions are the same elements in the 4 years. These elements are Al, Sc, Ti, V, Mn, Fe, Co, As, Zr, Ta, Th, and U. The three-moss species are utilized in 2015 and 2016. However, in 2014 and 2017, of three species, two were used (*P_schreberi* and *H_splendens; H_cupressiforme* and *P_schreberi*, respectively).

It is apparent that the concentrations of elements are slightly higher in *H. cupressiforme* than in *P. schreberi* and *H. splendens*. Nevertheless, the study showed that there were no significant differences in the mean values of elements. Therefore, we assumed that studied moss species accumulate

large-scale multielements from the atmospheric deposition equally, and there is no need for interspecies calibration (Fernández et al. 2015; Frontasyeva et al. 2020). Based on this assumption, these findings may be due to different levels of contamination in terms of localizations and sources of pollution.

The obtained concentrations of the trace elements in moss due to air deposition showed moderate variations; with the coefficients of variation (CV %) ranging from 30 to 85%, except for Cu, Mn, Ti, V, and As was calculated to be 186%, 162%, 105%, 104%, and 238%, respectively. The CV% values suggest significant variations in the mean values of the sampling profiles. The largest CV % value was observed for As and the smallest was for K (31.2%). Likewise, the values of skewness and kurtosis ranged from 0.6 and − 0.2 to 9.0 and 98 for Sr and Cl, respectively. Based on the fact that high values of CV (> 75%), positive skewness (> 0), and kurtosis (> 3) are likely to indicate the non-normal distribution and the impact of other factors on the concentrations of elements in moss samples (i.e., the elevated concentrations of elements that may lead to the existence of outliers, which in turn, will skew the data, from one hand. On the other hand, reduced collected samples) (Allajbeu et al. 2016; Hair et al. 2012; Zhou et al. 2017).

More information about the interaction between the mean values of the deposited concentrations in different moss species in different years was extracted by conducting Tukey test pairwise comparisons. The Tukey test was used to differentiate the differences of the mean values of the elements deposited in different moss species in different years. The results of the test are stipulated in Table 5. It is clear from the table that there is no significant difference in the mean values of the different moss species except *H. splendens* vs. *H. cupressiforme* ($p = 0.04$). The difference in the mean values of these two species may be explained by the unequal amounts of element deposition and accumulation. In addition, the nonuniform distribution of the contamination of the sampling localities. Furthermore, *H. splendens* was found mainly in relatively clean areas. Likewise, the same test was performed for investigating the mean differences in terms of sampling year. The results show that there are no significant differences except 2016 vs. 2015 ($p = 0.01$). This finding can be explained by the elevated concentrations in 2016.

The concentrations of the elements were compared in terms of median values with those published in the literature. The median values of the obtained results in the present research are in agreement with those published by Hristozova et al. (2019) in Bulgaria (2015/16, $n = 115$), Stafilov et al. (2018) in Macedonia (2015, $n = 72$), and Steinnes et al. (2017) in Norway (2015, $n = 229$). However, the median values of K, Mn, Zn, Ba, and Pb were higher than the corresponding values in Macedonia, Cu, I, Ba, Ce, Yb, Hf, W, and Pb in Bulgaria, and Mn, Zn, Se, and Ba in Norway, respectively. The comparison with the corresponding values reported for the aforementioned countries are given in Table 6.

Based on the obtained Box-Cox transformed matrix, the correlation matrix was constructed and the correlation coefficients were extracted. Having the correlation coefficients, we can investigate the degree of the chemical symmetries of the elements in the moss samples (Barandovski et al. 2015). The entire dataset was Box-Cox transformed prior to the correlation analysis (Box and Cox 1964). Next, the map of correlations between the elements after transformation is given in Fig. 4. Low correlations are displayed in hot colors (correlations close to − 1 are displayed in deep red color), while the high correlations are indicated in cold colors (correlations that are close to 1 are displayed in deep blue color). The matrix was built with the significance level $p = 0.05$ and the 0.95 confidence level. The correlation analysis demonstrates high positive correlations between the majorities of the measured elements except Cl and Cu. The correlation coefficients higher than 0.95 were observed for the following pairs of elements: Ti-V; Ce–Hf, Sm, Ta, Tb, U; Cr-Co, Fe, Ni; La-Co, Hf, Sm, Ta, Tb, U; Sc–Cr, Fe, Hf. The high correlation coefficient between the elements may involve common geochemical features. The correlation coefficient for U-Th is higher than 0.6.

Table 5 Tukey test was used to differentiate the differences of the mean values of the elements deposited in different moss species in different years

Moss species	Prob.	Sig.	Sampling year	Prob.	Sig.
H. splendens vs. *H. cupressiforme*	0.04	1	2015 vs. 2014	0.07	0
P. schreberi vs. *H. cupressiforme*	0.35	0	2016 vs. 2014	1.00	0
P. schreberi vs. *H. splendens*	0.79	0	2016 vs. 2015	0.01	1
			2017 vs. 2014	0.90	0
			2017 vs. 2015	0.62	0
			2017 vs. 2016	0.89	0

Sig. = 1 refers to a significant difference

Sig. = 0 refers to a nonsignificant difference

Table 6 Comparison of the median of the obtained concentration for the elements in moss with the corresponding values published by Stafilov et al. (2018) in Macedonia, Hristozova et al. (2019) in Bulgaria, and Steinnes et al. (2017) in Norway

Element	Georgia, 2014–2017 ($n=120$)		Macedonia, 2015 ($n=72$)		Bulgaria, 2015/2016 ($n=115$)		Norway, 2015 ($n=229$)	
	Median ± ASD	Range	Median	Range	Median	Range	Median	Range
Na	581 ± 235	101–3000	190	140–380	225	79–1560	210	60–800
Mg	3060 ± 770	1220–11,600	1900	1200–3800	2080	514–8550	1350	470–3280
Al	4295 ± 1500	759–24,500	2100	750–7400	2310	569–10,900	460	100–3050
Cl	185 ± 63.5	57.3–1080	ND	ND	78.8	16.6–861	ND	ND
K	5935 ± 1245	2030–15,000	6000	3100–14,000	5670	3250–14,200	3560	1770–6400
Ca	8255 ± 2050	4620–17,100	6900	3500–13,000	6630	606–14,200	3030	1820–7230
Sc	1.11 ± 0.4	0.17–6.58	ND	ND	0.41	0.10–3.13	0.09	0.02–1.4
Ti	349.5 ± 170.5	68.6–2100	ND	ND	143	46.4–764	24	6–152
V	9.4 ± 4.12	1.71–54	3.3	0.47–11	3.89	1.3–22.7	1.2	0.3–14
Cr	7.75 ± 2.65	2.04–39	5.7	1.8–31	2.73	0.219–25	0.7	0.2–17
Mn	141 ± 54.7	21.7–2530	160	33–510	180	39–551	400	40–1660
Fe	2725 ± 1050	404–14100	1700	510–4600	1190	376–7240	310	78–8125
Co	1.43 ± 0.61	0.23–8.12	0.6	0.16–2	0.59	0.197–3.29	0.2	0.06–23
Ni	5.56 ± 1.8	1.92–24.2	3.5	0.68–63	2.1	0.45–13.5	1.1	0.4–550
Cu	5.54 ± 2.31	0.13–143	4.6	3.0–8.3	7.36	3.2–46.88	4.2	1.8 370
Zn	28.85 ± 8.9	7.15–75.2	30	12–66	28	9–101	31	8–409
As	1.05 ± 0.56	0.18–83.3	0.54	0.13–1.4	0.45	0.20–3.57	0.13	0.04–4.72
Se	0.23 ± 0.09	0.068–0.65	ND	ND	0.2	0.008–0.67	0.3	0.009–2
Br	6.31 ± 1.46	2.33–25.2	ND	ND	2.8	1.2–9.4	ND	ND
Rb	10.55 ± 3.56	2.92–34.2	5.3	2.2–28	7.38	2.24–50.7	12.4	1.4–81
Sr	43.85 ± 12.85	17.2–157	25	6.5–220	25	11.3–122	13.6	3.8–60
Zr	10.55 ± 5.32	1.19–67.9	ND	ND	ND	ND	ND	ND
Mo	0.35 ± 0.1	0.14–2.1	0.17	0.08–0.51	ND	ND	ND	ND
Cd	5.57 ± 2.33	0.01–0.58	0.23	0.018–0.88	0.1	0.02–1.56	0.08	0.02–1.33
Sb	0.15 ± 0.07	0.049–1.36	ND	ND	0.11	0.04–0.51	0.07	0.007–0.38
I	0.16 ± 0.06	0.58–11.8	ND	ND	1.28	0.48–2.99	ND	ND
Cs	2.48 ± 1.09	0.036–2.67	ND	ND	0.207	0.0716–1.8	0.16	0.02–1.63
Ba	0.42 ± 0.19	4.98–365	42	9.7–180	46	14.2–309	25	5.3 130
La	51.3 ± 23.75	0.34–12	ND	ND	1.35	0.39–22.6	0.32	0.07–3.5
Ce	2.15 ± 0.91	0.31–21.7	ND	ND	2.4	0.5–29.2	0.61	0.10–4.78
Nd	3.75 ± 1.75	0.45–10.7	ND	ND	1.3	0.2–24.1	0.23	0.01–2.24
Sm	2.04 ± 0.87	0.031–2.7	ND	ND	ND	ND	0.05	0.004–0.38
Eu	0.34 ± 0.16	0.023–0.52	ND	ND	0.07	0.009–0.92	0.04	0.01–0.19
Tb	0.1 ± 0.04	0.011–0.31	ND	ND	0.03	0.005–0.42	0.01	< 0.001–0.09
Yb	0.05 ± 0.02	0.022–0.8	ND	ND	0.1	0.03–1.08	0.003	< 0.001–0.016
Hf	0.15 ± 0.07	0.041–1.81	ND	ND	0.16	0.04–1.44	ND	ND
Ta	0.27 ± 0.13	0.0069–0.28	ND	ND	0.04	0.009–0.28	ND	ND
W	0.06 ± 0.02	0.026–0.67	ND	ND	0.1	0.02–1.44	ND	ND
Pb	0.11 ± 0.04	0.18–19.1	4.9	2.2–14	10.7	3.72–102.8	0.05	0.001–0.4
Th	0.51 ± 0.23	0.063–2.9	ND	ND	0.39	0.09–2.8	0.03	0.007–1.5
U	0.16 ± 0.07	0.021–1.25	ND	ND	0.12	0.03–3.2	0.006	0.002–0.08

ASD absolute SD of median; *ND* not detected

Results of the pollution impact

The air quality was assessed using various approaches. The pollution extent was quantified within the most widely used approaches. For instance, the enrichment factor (EF), relative accumulation factor (RAF), pollution load index (PLI), potential ecological risk index (PER), and risk index (RI) were calculated for three different moss species.

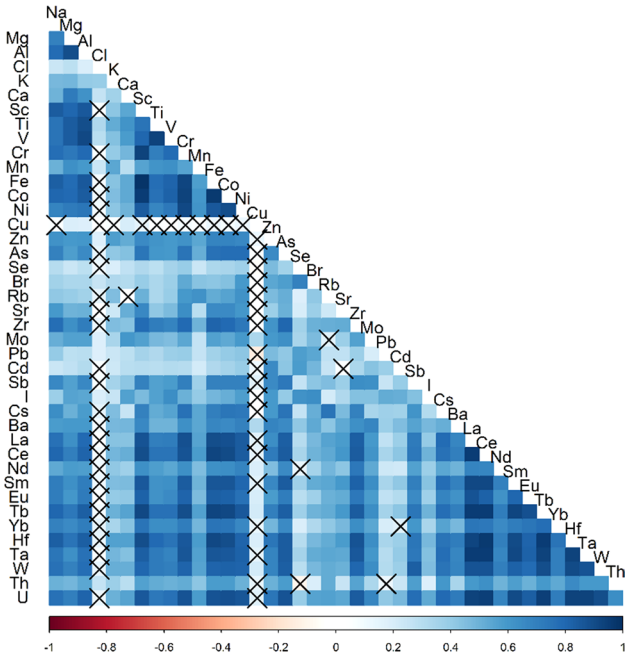

Fig. 4 Map of correlations between the elements of the entire initial data set based on the Box-Cox transformed data. A good correlation is observed after transformation. X stands for not significant. Low correlations are displayed with hot colors (correlations close to − 1 are displayed in deep red color), while the high correlations are indicated with cold colors (correlations that are close to 1 are displayed in deep blue color). The matrix was built with significant level $p = 0.05$ and 0.95 confidence level

The EF was calculated for the three-moss species, and the obtained results are given in Table 5SM for each single type and for all types. The highest mean values of EF were observed for Th and Zr. The mean value of EF for Th of 3.7 ± 2.27 with a minimum value of 0.54 was observed for location #101 (*H. cupressiforme* in 2016), and a maximum value of 10.79 was observed for location #42 (*H. splendens* in 2015). Likewise, the mean value of (EF) for Zr is 5.46 ± 2.24 with a range of 0.88 to 16.52. Based on the interpretation categories of enrichment factor, the obtained mean value of EF for Zr suggests a moderately severe enrichment. These peculiarities can be explained by the influence of the volcanic nature of the Lesser Caucasus Mountains (i.e., weathering). The elevated amounts of Zr can be described by the ratio Zr/Sc ratio, which was calculated for all moss species to be 10. This value is a good indicator of sedimentation recycling processes. Therefore, high amounts of Zr in moss species have a crustal association (felsic volcanic rocks and andesite) (Nagarajan et al. 2017).

A good agreement between the EF and RAF results was observed. RAF is given for As (375), Cu (187), and Mn (154), and they are considered quite high. In addition, the values for Sm, Ti, Zr, Ba, Hf, U, Sb, W, Sc, Th, Tb, and V range from 75 to 85. The high amount of As, Cu, and Mn are due to the influence of mining areas.

The pollution load index was calculated for the three-moss species. The spatial distribution of PLI results are mapped using GIS-technology based on the inverse distance weighting (IDW) method, as illustrated in Fig. 5. The figure demonstrates four peaks: (i) location #38 in Tsana and Koruldashi near Tskhenistsqali river, arsenic wastes dated back to the Soviet times (Safirova 2015; World Bank 2015), (ii) location #53, in the vicinity of Telavi. This location is characterized by the production of inert and construction materials, (iii) location #64, where the production of construction materials and asphalt is located, and (iv) location #12, mostly the elevated PLI in this location is due to the geological nature as it is composed of Pleistocene of andesitic-to-dacitic lava, and the volcanic mountain nature dominates. In addition, there are other locations that might pose a significant hazard to humans and environment viz., locations #44 and #97, where these locations are in the vicinity of Kutaisi Auto Mechanical Plant and Zestafoni Ferroalloy Plant; locations #82, #83, and #84, due to the influence of the coal mining in Tkibuli; and finally, locations #112, #113, and #114, where the Chiatura mine complex is located.

The potential ecological risk index (PER) was calculated for the toxic elements (Zn, As, Cr, Pb, Ni, Cu, and Cd). Based on the interpretation categories given in Table 4SM, that Zn, Cr, Pb, Ni, Cu do not pose any ecological risk, whereas As and Cd have a considerable PER. As has a quite considerable PER in 2015 and 2016, whereas Cd had a significant PER in 2017 with high uncertainty (Fig. 2SM A). This might be due to the substantial variations in concentrations of Mn (Mn mining in Chiatura) and Cu (gold-copper mining in Kazreti), which led to high uncertainty. Conversely, *H. cupressiforme* dominated in accumulation of As and Cd as clearly illustrated in Fig. 6. This can be explained by the impact of the mentioned mines.

The risk index was calculated and plotted for all moss species for each year (Fig. 2SM B). The figure illustrates the upper and lower margins of the risk index based on the interpretation given in Table 4SM. The figure depicts a considerable RI noticed in *H. cupressiforme* and *P. schreberi* in 2015 and 2016, while in 2014, significant RI by *H. cupressiforme* is noticed and most likely due to the reduced number of samples and, therefore, reflects significant uncertainty. To sum up, PER and RI are significant for *H. cupressiforme* in 2015 and 2016, mainly due to the elevated values of As and Cd.

Multivariate statistical analysis

Findings of discriminant analysis (DA)

The Sc-La-Th discriminatory diagram is illustrated in Fig. 7. For comparison purposes, the upper continental

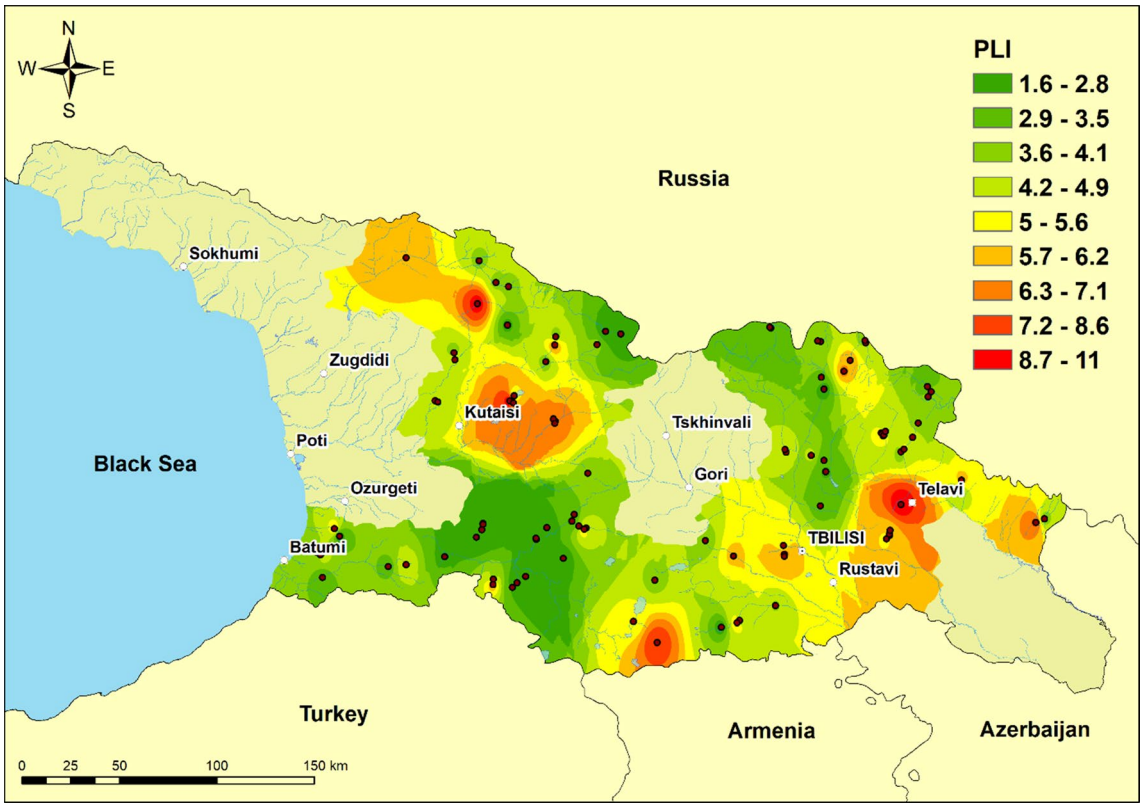

Fig. 5 Spatial distribution of the pollution load index PLI from the determined element over all sampling sites

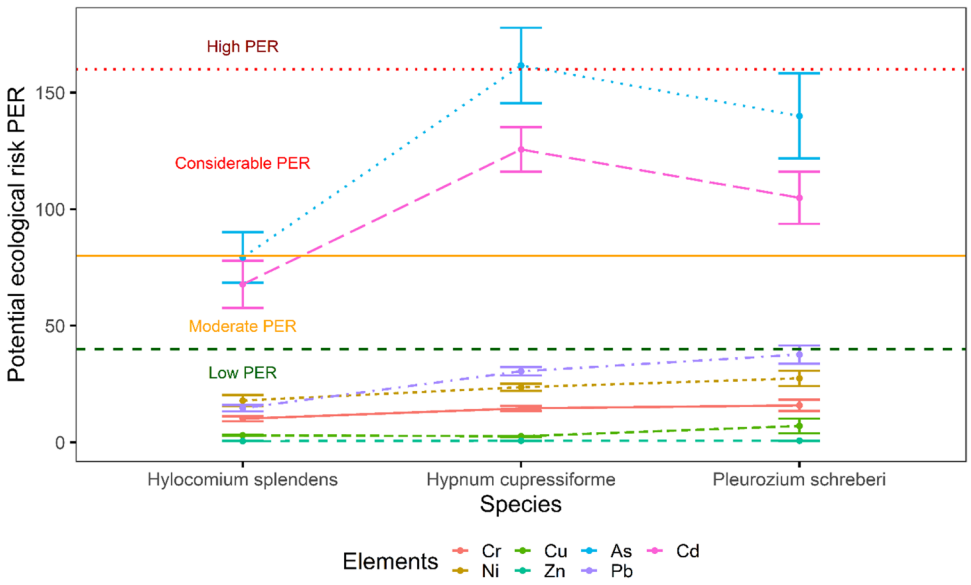

Fig. 6 Potential ecological index for selected elements accumulated by different moss species

crust (UCC) data reported by Rudnick and Gao (2014), the corresponding values in Norway reported by Steinnes et al. (2017), and reference plant values reported by Markert (1992) are added. The ternary diagram depicts the symmetrical distribution of the elements near the vicinity of (UCC) and quite close to corresponding values obtained in Norway by Steinnes et al. (2017). Contrariwise, the distribution of the elements is slightly far from the reference plant values. These findings can be explained by the significant association of crustal amounts as the three-moss species are allocated in the vicinity of (UCC) in the ternary diagram.

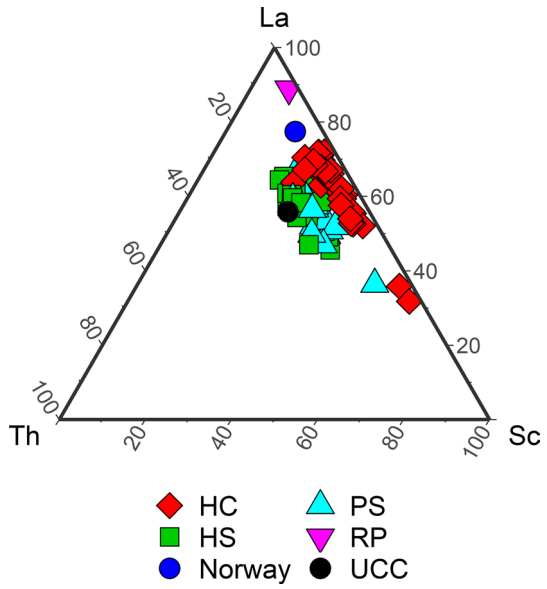

Fig. 7 Sc-La-Th discriminatory diagram depicting the symmetrical distribution of elements near the UCC. For comparison, the UCC data by Rudnick and Gao (2014), the corresponding values in Norway by Steinnes et al. (2017), and reference plant data by Markert (1992) also are shown

Findings of the principal component analysis

The first three principal component analysis (PCA) accounted for 8.29 (28.59%), 4.34 (14.95%), and 2.4 (8.3%) of the eigenvalues and percentage of variance (in parentheses), respectively. The first three dimensions of the PCA express 51.86% of the total dataset cumulative percentage of the variance. Based on the two first PCAs, the data can be sufficiently explained.

On the basis of the K-mean method, the first two (PCAs) of the variables were plotted and grouped as illustrated in the biplot of the Q-mode (PCAs plot for variables) in Fig. 8A. The figure revealed three clusters, which can be summarized as; the first cluster includes seven elements: Na, Al, Sc, Ti, V, Fe, and Co. This group of elements represents the geogenic origin of elements with an anthropogenic association. The second group consists of elements of common geochemical traits: e.g., Th:U, Hf:Zr, and rare earth elements, such as Eu, La, and Ce. A considerable association of As in this cluster was mainly due the influence of Tsana and Uravi arsenic mining sites situated in the Ambrolauri and Lentekhi municipalities (Chirakadze et al. 2016). Therefore, this cluster is categorized as a mixture of geogenic and anthropological elements. While the third cluster represents 12 elements (Mg, Cl, K, Ca, Mn, Ni, Zn, Br, Rb, Sr, I, and Ba). It is obvious that Br and I are transported from the sea by weathering where Adjara is located close to the Black Sea, while the others are mainly crustal elements enhanced by anthropogenic influence. In particular, elevated amounts of Mn suggest the significant contribution of Chiatura manganese mining in Imereti.

Similarly, with a confidence level of 95%, the first two PCAs for categorization of sampling sites (R mode) are

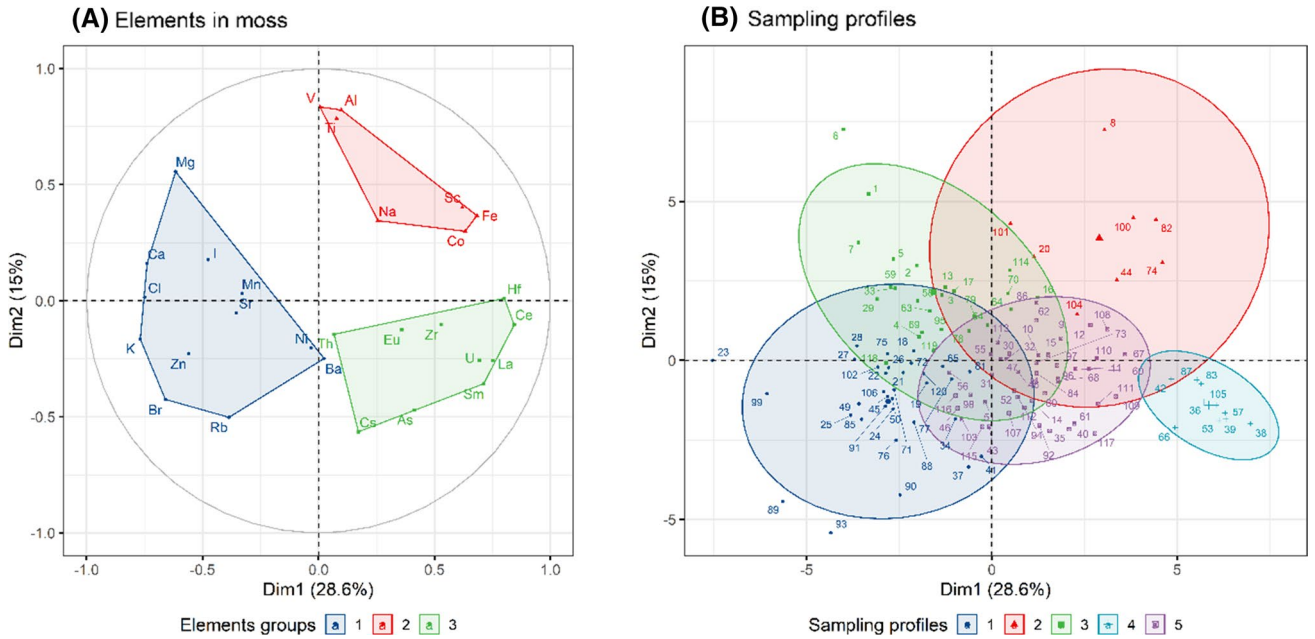

Fig. 8 Biplot of the first two PCAs of the moss species studied ($n = 120$) and selected elements ($n = 29$) illustrating clusters 3 and 5 for elements and sampling sites, respectively

plotted and illustrated in Fig. 8B. The biplot depicts five clusters, and these clusters are grouped in terms of common traits in the sampling sites. The five clusters could be described as follows: the first group contains 44 locations, and among these, some have significant contributions (i.e., 112 and 113). These locations are characterized by Mn mining areas. The second cluster contains ten locations. The highest contribution of As was observed in location #87 where As mining areas and the location #38 is located near to Tskhenistsqali river—Tsana and Koruldashi (places with arsenic-containing waste). In addition, locations #53 is close to area of production of inert materials in Kakheti region, environs of city Telavi. The third cluster groups 25 locations and includes the location of the highest concentration of Mn (#114) as it is close to Mn mining area. The fourth group includes 33 neighboring sampling sites, and it overlaps with almost all the other clusters. Based on the characterization of the locations, there are no potential sources of pollution in their vicinity. The fifth cluster has locations with no potential sources of pollution as well.

The results of PCA showed clusters with neighboring sampling profiles, as it is obviously from the order of the profiles in each cluster. In addition to the previous deliberations and for a better understanding on which basis the clusters of sampling sites are grouped, a brief description of the climate regions is given. The climate in Georgia can be classified into three regions: maritime subtropical humid; moderately humid subtropical; and transitional subzone from moderately humid subtopic to Middle East highland dry subtropic climate (Tielidze et al. 2019). Furthermore, it is quite clear from the map given by Tielidze et al. (2019) for the climate types of Georgia and the transitional borders from each type to another that there are five different latitudinal and climate zones, which in turn form the clusters in Fig. 8B with some overlapping. To summarize, it can be stated that the wind direction, the significant role of Great and Lesser Caucasus Mountains, and Eastern and Western Georgia climatic zones significantly contribute to the weathering and transportation of elements from the sea and/or mountainous zones. Eventually, all of these factors affect the degree of accumulation of trace elements by moss species from the atmosphere, and the association of crustal rocks and soil reveals the significant contribution of geogenic elements, which in our case is not avoidable.

Conclusions

This study achieved its primary objective of reporting baseline data on the accumulated trace metals in different moss species in Georgia. The normalized concentrations of Al, Sc, Ti, V, Cr, Fe, Co, As, Se, Zr, Pb, Cd, Hf, Th, U, and rare earth elements (La, Ce, Sm, Eu, Tb, and Yb) are significantly high. Furthermore, the normalized concentrations of the elements that are deposited in *H. cupressiforme* are slightly higher than in *P. schreberi* and *H. splendens*. The intercorrelation findings suggest that there are no significant differences between the mean concentrations of the elements in terms of the year of sampling and the type of species except for *H. cupressiforme* vs. *H. splendens* in 2016 vs. 2015, respectively.

Discriminant analysis shows that there is a considerable association of crustal concentrations due to soil weathering. In addition, based on (PCA) analysis three clusters of elements with symmetrical geochemical features were represented. The first group is including the elements with common features and have both geogenic and anthropologic provenance, namely, Na, Al, Sc, Ti, V, Fe, and Co. The anthropological contribution mostly due to the Zestafoni Ferroalloy Plant and Kutaisi Auto Mechanical Plant. Likewise, the second group are the paired elements with geochemical symmetry, such as Th:U, Hf:Zr, and rare earth elements, such as Sm, Eu, La, and Ce are well correlated. A considerable association of As was noticed and mostly due to the Tsana and Uravi arsenic mining sites situated in the Ambrolauri and Lentekhi Municipalities. The third group is a mixture of sea elements (Br, I) due to the Black Sea aerosol weathering and other natural elements with concentrations increased by anthropological impacts as Mn due to the Chiatura manganese mining in Imereti. Similarly, five clusters were formed and emphasize the great similarity with the different latitudinal and climate zones of Georgia. Therefore, the association of crustal rocks and soil reveals the significant contribution of crustal geogenic elements, which cannot be avoided in our case.

The EF showed moderately severe enrichment of *H. splendens* with Zr, and it indicates a significant amount of zircon, which is a good tracer during the sorting and recycling processes. Thus, the source of Zr in the moss samples is felsic volcanic rocks or andesite, mostly due to volcanic mountainous zones in Southern Georgia. In addition, the EF values for Ti, Sc, and Th show that these elements are minor enriched. The pollution load index PLI was mapped, and four peak regions were identified (#38, 53, 64, and 12). The potential ecological risk index PER and the risk index RI are significant in 2015 and 2016 for *H. cupressiforme* with the highest contribution from the elevated values of As and Cd caused by arsenic wastes in Tsana and Koruldashi and emission from the Zestafoni Ferroalloy Plant, respectively. Having the first dataset of characterization of inorganic air metal pollution in Georgia is an effective tool that might help the regulatory bodies to set the necessary laws and rules that control the emission of toxic elements in the atmosphere.

Acknowledgments The authors acknowledge the grant of the Plenipotentiary of Georgia at the Joint Institute for Nuclear Research (Order

#37 of 22.01.2020). The authors express their gratitude to Prof. Richard Hoover (NASA Marshall Space Flight Center, Huntsville, Huston, USA) for editing the English language.

References

Abdusamadzoda D, Abdushukurov DA, Duliu OG, Zinicovscaia I, Yushin NS, Frontasyeva MV (2019) Investigations of the atmospheric deposition of major and trace elements in Western Tajikistan by using the hylocomium splendens moss as bioindicators. Arch Environ Contam Toxicol. https://doi.org/10.1007/s00244-019-00687-w

Abrahim GMS, Parker RJ (2008) Assessment of heavy metal enrichment factors and the degree of contamination in marine sediments from Tamaki Estuary, Auckland, New Zealand. Environ Monitor Assess 136:227–238. https://doi.org/10.1007/s10661-007-9678-2

Acosta JA, Gabarrón M, Faz A, Martínez-Martínez S, Zornoza R, Arocena JM (2015) Influence of population density on the concentration and speciation of metals in the soil and street dust from urban areas. Chemosphere 134:328–337. https://doi.org/10.1016/j.chemosphere.2015.04.038

Allajbeu S, Yushin NS, Qarri F, Duliu OG, Lazo P, Frontasyeva MV (2016) Atmospheric deposition of rare earth elements in Albania studied by the moss biomonitoring technique, neutron activation analysis and GIS technology. Environ Sci Pollut Res 23:14087–14101. https://doi.org/10.1007/s11356-016-6509-4

Avkopashvili G, Avkopashvili M, Gongadze A, Tsulukidze M, Shengelia E (2017) Determination of Cu, Zn and Cd in soil, water and food products in the vicinity of RMG gold and copper mine, Kazreti, Georgia. Ann Agrarian Sci 15:269–272. https://doi.org/10.1016/j.aasci.2017.05.001

Azimi S, Ludwig A, Thévenot DR, Colin J-L (2003) Trace metal determination in total atmospheric deposition in rural and urban areas. Sci Total Environ 308:247–256. https://doi.org/10.1016/S0048-9697(02)00678-2

Badawy WM, Ghanim EH, Duliu OG, El Samman H, Frontasyeva MV (2017) Major and trace element distribution in soil and sediments from the Egyptian central Nile Valley. J Afr Earth Sci 131:53–61. https://doi.org/10.1016/j.jafrearsci.2017.03.029

Badawy WM, El-Taher A, Frontasyeva MV, Madkour HA, Khater AEM (2018) Assessment of anthropogenic and geogenic impacts on marine sediments along the coastal areas of Egyptian Red Sea. Appl Radiat Isotopes 140:314–326. https://doi.org/10.1016/j.apradiso.2018.07.034

Badawy WM, Duliu OG, Frontasyeva MV, El-Samman H, Mamikhin SV (2020) Dataset of elemental compositions and pollution indices of soil and sediments: Nile River and delta -Egypt Data in Brief 28. https://doi.org/10.1016/j.dib.2019.105009

Barandovski L, Frontasyeva MV, Stafilov T, Šajn R, Ostrovnaya TM (2015) Multi-element atmospheric deposition in Macedonia studied by the moss biomonitoring technique. Environ Sci Pollut Res 22:16077–16097. https://doi.org/10.1007/s11356-015-4787-x

Boquete MT, Fernández JA, Aboal JR, Carballeira A (2011) Are terrestrial mosses good biomonitors of atmospheric deposition of Mn? Atmos Environ 45:2704–2710. https://doi.org/10.1016/j.atmosenv.2011.02.057

Box GEP, Cox DR (1964) An analysis of transformations. J Roy Stat Soc: Ser B (Methodol) 26:211–243. https://doi.org/10.1111/j.2517-6161.1964.tb00553.x

Brunekreef B, Holgate ST (2002) Air pollution and health. Lancet 360:1233–1242. https://doi.org/10.1016/S0140-6736(02)11274-8

Carballeira A, Couto JA, Fernández JA (2002) Estimation of background levels of various elements in terrestrial mosses from Galicia (NW Spain). Water Air Soil Pollut 133:235–252. https://doi.org/10.1023/A:1012928518633

Caruso BS, Mirtskhulava M, Wireman M, Schroeder W, Kornilovich B, Griffin S (2012) Effects of manganese mining on water quality in the Caucasus Mountains, Republic of Georgia. Mine Water Environ 31:16–28. https://doi.org/10.1007/s10230-011-0163-3

Chen CW, Kao CM, Chen CF, Di Dong C (2007) Distribution and accumulation of heavy metals in the sediments of Kaohsiung Harbor. Taiwan. Chemosphere 66:1431–1440. https://doi.org/10.1016/j.chemosphere.2006.09.030

Chirakadze A et al (2016) Arsenic pollution of soils and morbidity prevalence in Racha-Lower Svaneti district of Georgia. Int J Glob Warming 10:92–114

Ergin M, Saydam C, Başztürk Ö, Erdem E, Yörük R (1991) Heavy metal concentrations in surface sediments from the two coastal inlets (Golden Horn Estuary and İzmit Bay) of the northeastern Sea of Marmara. Chem Geol 91:269–285. https://doi.org/10.1016/0009-2541(91)90004-B

Fernández JA, Boquete MT, Carballeira A, Aboal JR (2015) A critical review of protocols for moss biomonitoring of atmospheric deposition: sampling and sample preparation. Sci Total Environ 517:132–150. https://doi.org/10.1016/j.scitotenv.2015.02.050

Frontasyeva M, Pavlov SS (2005) Scientific reviews: radioanalytical investigations at the IBR-2 reactor in Dubna. Neutron News 16:24–27. https://doi.org/10.1080/10448630500454387

Frontasyeva M, Harmens H, Uzhinskiy A, Chaligava O (2020) Mosses as biomonitors of air pollution: 2015/2016 survey on heavy metals, nitrogen and POPs in Europe and beyond

Gambashidze GO, Urushadze TF, Blum WE, Mentler AF (2014) Heavy metals in some soils of Western Georgia. Eurasian Soil Sci 47:834–843. https://doi.org/10.1134/S1064229314080031

Goryainova Z, Vuković G, Urošević MA, Vergel K, Ostrovnaya T, Frontasyeva M, Zechmeister H (2016) Assessment of vertical element distribution in street canyons using the moss Sphagnum girgensohnii: a case study in Belgrade and Moscow cities. Atmos Pollut Res 7:690–697. https://doi.org/10.1016/j.apr.2016.02.013

Hair JF, Sarstedt M, Pieper TM, Ringle CM (2012) The use of partial least squares structural equation modeling in strategic management research: a review of past practices and recommendations for future applications. Long Range Plan 45:320–340. https://doi.org/10.1016/j.lrp.2012.09.008

Hakanson L (1980) An ecological risk index for aquatic pollution control: a sedimentological approach. Water Res 14:975–1001. https://doi.org/10.1016/0043-1354(80)90143-8

Hallinan JS (2012) Chapter 2—Data mining for microbiologists. In: Harwood C, Wipat A (eds) Methods in microbiology, vol 39. Academic Press, London, pp 27-79. https://doi.org/10.1016/B978-0-08-099387-4.00002-8

Hamilton NE, Ferry M (2018) ggtern: Ternary diagrams using ggplot2 2018 87:17 https://doi.org/10.18637/jss.v087.c03

Harmens H, Mills G, Hayes F, Sharps K, Frontasyeva M (2015) Air pollution and vegetation: ICP Vegetation annual report 2014/2015. ICP Vegetation Programme Coordination Centre, CEH Bangor, UK. https://doi.org/10.13140/RG.2.1.1294.9200

Hassanien MA (2011) Atmospheric heavy metals pollution: exposure and prevention policies in Mediterranean basin vol 1. Environmental Heavy Metal Pollution and Effects on Child Mental Development. NATO Science for Peace and Security Series C: Environmental Security. Springer, Dordrecht. https://doi.org/10.1007/978-94-007-0253-0_17

Hristozova G, Marinova S, Svozilík V, Nekhoroshkov P, Frontasyeva MV (2019) Biomonitoring of elemental atmospheric deposition: spatial distributions in the 2015/2016 moss survey in Bulgaria. J Radioanalytical Nucl Chem. https://doi.org/10.1007/s10967-019-06978-9

Kampa M, Castanas E (2008) Human health effects of air pollution. Environ Pollut 151:362–367. https://doi.org/10.1016/j.envpol.2007.06.012

Karuppasamy MP, Qurban MA, Krishnakumar PK, Mushir SA, Abuzaid N (2017) Evaluation of toxic elements As, Cd, Cr, Cu, Ni, Pb and Zn in the surficial sediments of the Red Sea (Saudi Arabia). Mar Pollut Bull 119:181–190. https://doi.org/10.1016/j.marpolbul.2017.04.019

Kowalska J, Mazurek R, Gąsiorek M, Setlak M, Zaleski T, Waroszewski J (2016) Soil pollution indices conditioned by medieval metallurgical activity – a case study from Krakow (Poland). Environ Pollut 218:1023–1036. https://doi.org/10.1016/j.envpol.2016.08.053

Kowalska JB, Mazurek R, Gąsiorek M, Zaleski T (2018) Pollution indices as useful tools for the comprehensive evaluation of the degree of soil contamination–A review. Environ Geochem Health 40:2395–2420. https://doi.org/10.1007/s10653-018-0106-z

Lê S, Josse J, Husson F (2008) FactoMineR: an R package for multivariate analysis. J Stat Softw 25:18. https://doi.org/10.18637/jss.v025.i01

Lomsadze Z, Makharadze K, Pirtskhalava R (2016) The ecological problems of rivers of Georgia (the Caspian Sea basin). Ann Agrarian Sci 14:237–242. https://doi.org/10.1016/j.aasci.2016.08.009

Lv J, Liu Y, Zhang Z, Zhou R, Zhu Y (2015) Distinguishing anthropogenic and natural sources of trace elements in soils undergoing recent 10-year rapid urbanization: a case of Donggang, Eastern China. Environ Sci Pollut Res 22:10539–10550. https://doi.org/10.1007/s11356-015-4213-4

Madadzada AI, Badawy WM, Hajiyeva SR, Veliyeva ZT, Hajiyev OB, Shvetsova MS, Frontasyeva MV (2019) Assessment of atmospheric deposition of major and trace elements using neutron activation analysis and GIS technology: Baku—Azerbaijan. Microchem J 147:605–614. https://doi.org/10.1016/j.microc.2019.03.061

Markert B (1992) Establishing of reference plant for inorganic characterization of different plant-species by chemical fingerprinting. Water Air Soil Pollu 64:533–538. https://doi.org/10.1007/Bf00483363

Nagarajan R, Armstrong-Altrin JS, Kessler FL, Jong J (2017) Chapter 7—Petrological and geochemical constraints on provenance, paleoweathering, and tectonic setting of clastic sediments from the Neogene Lambir and Sibuti formations, Northwest Borneo. In: Mazumder R (ed) Sediment Provenance. Elsevier, pp 123–153. https://doi.org/10.1016/B978-0-12-803386-9.00007-1

R Core Team (2016) R: A language and environment for statistical computing. R Foundation for Statistical Computing, Vienna

Reimann C, de Caritat P (2005) Distinguishing between natural and anthropogenic sources for elements in the environment: regional geochemical surveys versus enrichment factors. Sci Total Environ 337:91–107. https://doi.org/10.1016/j.scitotenv.2004.06.011

Reimann C, Filzmoser P (2000) Normal and lognormal data distribution in geochemistry: death of a myth. Consequences for the statistical treatment of geochemical and environmental data. Environ Geol 39:1001–1014. https://doi.org/10.1007/s002549900081

Rudnick RL, Gao S (2014) Composition of the continental crust A2—Holland, Heinrich D. In: Turekian KK (ed) Treatise on Geochemistry (Second Edition). Elsevier, Oxford, pp 1-51. https://doi.org/10.1016/b978-0-08-095975-7.00301-6

Safirova E (2015) The mineral industry of Georgia

Saitanis CJ, Frontasyeva MV, Steinnes E, Palmer MW, Ostrovnaya TM, Gundorina SF (2013) Spatiotemporal distribution of airborne elements monitored with the moss bags technique in the Greater Thriasion Plain, Attica, Greece. Environ Monitor Assess 185:955–968. https://doi.org/10.1007/s10661-012-2606-0

Salim Akhter M, Madany IM (1993) Heavy metals in street and house dust in Bahrain. Water Air Soil Pollut 66:111–119. https://doi.org/10.1007/bf00477063

Shapiro SS, Wilk MB (1965) An analysis of variance test for normality (complete samples). Biometrika 52:591–611. https://doi.org/10.1093/biomet/52.3-4.591

Stafilov T, Šajn R, Barandovski L, Andonovska KB, Malinovska S (2018) Moss biomonitoring of atmospheric deposition study of minor and trace elements in Macedonia. Air Qual Atmos Health 11:137–152. https://doi.org/10.1007/s11869-017-0529-1

Steinnes E, Rambæk JP, Hanssen JE (1992) Large scale multi-element survey of atmospheric deposition using naturally growing moss as biomonitor. Chemosphere 25:735–752. https://doi.org/10.1016/0045-6535(92)90435-T

Steinnes E, Hanssen JE, Rambaek JP, Vogt NB (1994) Atmospheric deposition of trace-elements in Norway—temporal and spatial trends studied by moss analysis. Water Air Soil Poll 74:121–140. https://doi.org/10.1007/Bf01257151

Steinnes E, Rühling Å, Lippo H, Mäkinen A (1997) Reference materials for large-scale metal deposition surveys. Accreditation Qual Assurance 2:243–249. https://doi.org/10.1007/s007690050141

Steinnes E, Uggerud HT, Pfaffhuber KA, Berg T (2017) Atmospheric deposition of heavy metals in Norway. National moss survey 2015. NILU – Norwegian Institute for Air Research P.O. Box 100, 2027 Kjeller

Tessier L, Boisvert JL (1999) Performance of terrestrial bryophytes as biomonitors of atmospheric pollution. A review. Toxicol Environ Chem 68:179–220. https://doi.org/10.1080/02772249909358655

Tielidze L, Trapaidze V, Matchavariani L, Wheate R (2019) Climate, hydrography, and soils of Georgia. In: Tielidze L (ed) Geomorphology of Georgia. Springer International Publishing, Cham, pp 15-34. https://doi.org/10.1007/978-3-319-77764-1_2

Urushadze TF, Ghambashidze G, Blum WEH, Mentler A (2007) Soil Contamination with Heavy Metals in Imereti Region (Georgia) Bull Georgian National Acad f Sci 175

Varol M (2011) Assessment of heavy metal contamination in sediments of the Tigris River (Turkey) using pollution indices and multivariate statistical techniques. J Hazard Mater 195:355–364. https://doi.org/10.1016/j.jhazmat.2011.08.051

Westen CJ et al. (2012) Atlas of natural hazards and risk in Georgia

Wickham H (2016) ggplot2: Elegant graphics for data analysis. Springer-Verlag, New York

World Bank (2015) Georgia country environmental analysis: institutional, economic, and poverty aspects of Georgia's road to environmental sustainability

Yekeen TA et al (2016) Assessment of health risk of trace metal pollution in surface soil and road dust from e-waste recycling area in China. Environ Sci Pollut Res 23:17511–17524. https://doi.org/10.1007/s11356-016-6896-6

Zhou X, Chen Q, Liu C, Fang Y (2017) Using moss to assess airborne heavy metal pollution in Taizhou, China. Int J Environ Res Public Health 14:430. https://doi.org/10.3390/ijerph14040430